

S E S S I O N I I I

OBSERVED ACTIVITY IN RELATED OBJECTS

: THE SUN

: RS CVn BINARIES

: CONTACT BINARIES

: T Tau AND OTHER ACTIVE STARS

FLARES ON THE SUN : SELECTED RESULTS FROM SMM.

G.M.Simnett
Department of Space Research
University of Birmingham
Birmingham B15 2TT

1. INTRODUCTION

Observationally the study of solar flares has reached the stage where intensity-time distributions of emission over broad and resolved regions of the electromagnetic spectrum are obtained for spatially resolved parts of the flare. Polarization measurements add an important diagnostic tool in some wavebands but we shall not report on these here. In the optical band good ground based observations have been available for many years, whereas in the UV, soft X-ray and hard X-ray (> 5 keV) bands recent spacecraft have greatly extended the data base. Good high resolution maps are being made in the microwave region with the ground based VLA. We are now at the point where significant progress into understanding the flare problem has been made, and will continue to be made, during the current solar maximum. This coincides with the development of soft X-ray instruments sensitive enough to detect transient and quiescent emission from flare stars, particularly red dwarfs in the solar neighbourhood (e.g. Kahn et al, 1979, Haisch et al, 1980) which previously had only been detected in the optical and radio wavebands. In the light of this important milestone it is appropriate to review the current advances being made with the Solar Maximum Mission (SMM) data set on solar flares and to examine how they can further the interpretation of flare star behaviour. We first indicate the physical parameters which can be readily deduced from the observations, and then show how SMM provides sufficiently well co-ordinated measurements for real advances to be made.

2. THE PHYSICAL FRAMEWORK OF FLARES

A typical solar flare starts with a slow increase in temperature and emission measure from the subsequent flare site. The energy source is in the strong magnetic field associated with the sunspot groups within which flares almost invariably occur. Generally a bipolar magnetic flux tube is close to the source of energy release, and observations of the post-flare state often indicate an arcade of loops stretching into the low corona. Following the pre-flare increase by some minutes is the

main impulsive phase, when the hard X-rays are emitted. In this phase the bulk of the flare energy resides in the kinetic energy of non-thermal electrons > 10 keV and, perhaps more significantly, ions; the energy is relatively invisible to us if the latter dominates. Electrons which encounter a high density medium such as the chromosphere, immediately radiate via non-thermal bremsstrahlung. The resultant X-ray spectrum generally suggests a power law distribution of electron energies, $dJ(E)/dE \propto E^{-\gamma}$, where E is the energy in keV. The relationship of the index γ to the observed X-ray spectrum depends on the thick or thin target nature of the emission, the former appropriate for an electron beam hitting the chromosphere and the latter appropriate for an electron beam trapped in, or escaping from, the corona (Lin & Hudson, 1976). Where electrons encounter suitable magnetic fields in the relative absence of matter, such as at the top of a magnetic arch, they produce microwave radiation. Similarities between hard X-ray and microwave intensity-time profiles suggest that these emissions are from different fractions of the same population of electrons. The ions, if sufficiently energetic ($> \text{few MeV}$) may produce nuclear gamma rays, but otherwise they remain invisible, contributing only to the thermal energy content of the ambient medium. During the impulsive phase intensity fluctuations are rapid ($< 1\text{s}$) which makes unambiguous interpretation of the flare difficult.

Both electron and ion populations create a hot thermal plasma as they stop. Moore et al (1980) showed that the most significant fraction of the total flare energy resides in this plasma during the slow decay phase. The plasma is contained in a magnetic flux tube thought to be approximately in pressure equilibrium; therefore the energy is dissipated either through conduction or radiation. Moore et al (1980) derive the characteristic cooling times, τ , of a plasma in the 10^7K region :

$$\text{conduction dominated } \tau_c \cong 4 \times 10^{-10} L^2 n_e^{-5/2} \text{ s} \quad (1)$$

$$\text{radiation dominated } \tau_r \cong 10^7 T n_e^{-1} \text{ s} \quad (2)$$

where T is the temperature (K), n_e the electron density (cm^{-3}) and L the length (cm) of the flux tube. In the decay phase temperatures and emission measures may be derived from the observations. The emission measure Y is given by :

$$Y = \int n_e n_i dV \cong \int n_e^2 dV \quad \text{cm}^{-3} \quad (3)$$

where n_i is the ion density, assumed equal to n_e , and V is the volume (cm^3). In some instances the differential (with respect to temperature) emission measure can be derived from line spectra; however analysis of the latter to determine flare parameters is a complex and evolving science, beyond the scope of this review. At higher energies, ≥ 10 keV, the thermal bremsstrahlung continuum dominates, and Crannell et al (1978) derive the following :

$$\frac{dN(E)}{dE} = 1.3 \times 10^3 \cdot Y \cdot e^{-E/aT} \cdot E^{-1.4} \cdot T^{-0.1} \quad (4)$$

where $N(E)$ is the measured photon spectrum and aT is the temperature in keV. Thus the measured photon spectrum can be used to determine the temperature and emission measure of the thermal plasma.

Consideration of (1)-(4) shows that the situation, as described, is close to being defined; the uncertainties are the choice between (1) and (2) as to the cooling mechanism, the definition of the volume, and the observational data. In practice other factors such as additional energy input and lack of stability in the principal flare loop are a complication.

One parameter which may link the impulsive and thermal phases is the total energy in the flare. During the impulsive phase integration of the electron spectrum, derived from the hard X-ray spectrum, gives a lower limit to the energy (the balance being in the ions), while in the thermal phase the energy of the plasma, Q , is given by:

$$Q = 3 Y k T n_e^{-1} \text{ erg} \quad (5)$$

This immediately sets a constraint on the magnetic field, for if the plasma is to be contained, the magnetic pressure $B^2/8\pi$ must exceed the thermal pressure $n_e kT$. Microwave emission is a function of the electron spectrum and the magnetic field. It can be seen from (1)-(5) that if the observations are of high quality and co-ordinated, then some real limits may be placed on a number of flare parameters. The thermal phase is better understood, and it is this phase alone that can, at the current time, be studied in flare stars.

In so far as they are observed, flares in nearby stars involve energy of a different order of magnitude than even the largest solar flares - 10^{35} erg compared with $\approx 10^{32}$ erg. The largest estimate for a stellar flare in the optical band is 6×10^{34} erg from YZ CMi on Jan 19, 1969 (Kunkel, 1969). Despite the high energy, they have such a short rise time that they have to be local phenomena, rather than sudden expansions of the star's envelope. For example, UV Cet increased its output by a factor of 420 in 31s, or $2^{m.8}/s$, during a flare on Sept 22, 1974 (Jarrett and Gibson, 1975). They do not radiate strongly in X-rays, and only recently have soft X-ray flares been detected from some of the nearer red dwarfs, ATMic (dM4.5e), ADLeo (dM3.5e) and Prox. Cen (dM5e) (Kahn et al, 1979; Haisch et al, 1980).

If the understanding of stellar flares is to benefit from solar flare studies, we must discover how to scale from solar conditions to those in the dwarf. Kahler and Shulman (1972) used the ratio of the soft X-ray (1-20 Å) luminosity to optical luminosity as seen in a "typical" solar flare. However, this is quite inappropriate for stellar flares; in UV Cet the soft X-ray luminosity is an order of magnitude too low when compared with the Sun. Mullan (1976) showed that the relative power in the X-ray/optical wavebands is related to the

radiated/conducted energy loss from the hot plasma. Under the assumption that conductive losses exceed radiative losses, and taking relative dimensions into account, he argues that X-ray luminosities on red dwarfs should be an order of magnitude, or more, lower than solar equivalents. However, we must remember that the theoretical treatments leading to (1) and (2) are relatively imprecise.

The e-folding decay time of a flare appears to be constant for a given star (Kunkel, 1975). This is not true for solar flares, although some simple compact flares have a rapid, ~ 1 m, decay time for the soft X-rays. In more complex flares, which are generally larger in area, the decay time at a given wavelength is very inhomogeneous. Fig. 1 shows the 3.5-8.0 keV X-ray intensity-time history of a flare seen by the Hard X-ray Imaging Spectrometer (HXIS) on SMM. The upper left panel shows the complete flare, with the gradual onset before this impulsive phase inset on an expanded intensity scale. The other panels show the time line for different parts of the flare. In all cases the decay of specific parts is much faster than the decay of the whole. The rise time also shows wide differences. This is a caution regarding the use of simple radiation and conduction theory for a complex flare as the energy is redistributed within the flare rather than escaping to an infinite heat sink (the photosphere for conductive losses and space for radiative losses). The uniformity of stellar flares may point to a simple, dominant flare scenario on the red dwarfs, paradoxically involving larger magnetic structures (to explain the high total energy). On intrinsically brighter stars, the magnetic structures are on a smaller scale and are more complex, perhaps leading to very efficient energetic particle acceleration and correspondingly higher hard X-ray luminosity. On the Sun the impulsive hard X-rays are produced primarily by non-thermal electrons not by high temperature thermal plasmas.

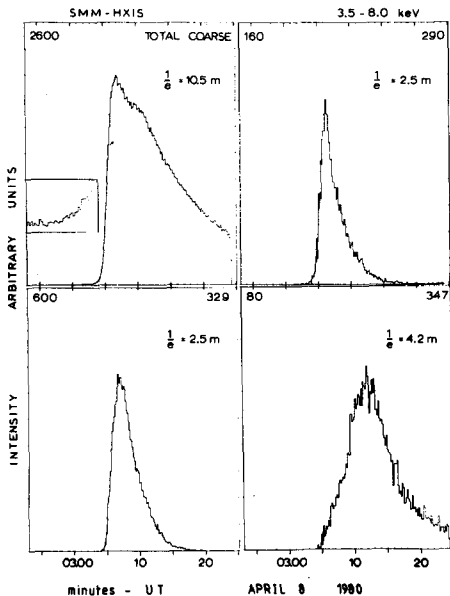


Figure 1. Soft X-ray intensity-time histories from a flare on April 8. Clockwise from upper left: the total flare with the onset magnified inset; 20" NE of the flare core; the flare core; 20" SW of the flare core. The number in the upper left corner of each panel is the intensity at the top of that panel.

3. THE RESULTS FROM SMM

NASA launched SMM on Feb 14, 1980 from Cape Canaveral, Florida. It represented the most comprehensive set of instruments ever assembled to study the active Sun. They monitored electromagnetic radiation from the optical to the γ ray part of the spectrum, with high time resolution, good spectral resolution and in some regions high spatial resolution (10" or better). The payload is described in Solar Physics 65, 1980; the first results were published in Ap.J.Lett. 244, 1981; and a review of the significant scientific achievements during the period of full operation, up to December 1980 was given by Simnett (1981).

The strength of SMM was its ability to study the impulsive phase simultaneously with the full complement of instruments. It is not, surprising, therefore, that the most definitive new results have emerged from these studies. Prior to launch it was suspected that the hard X-rays, >20 keV, did not exhibit faster variations than about 1 s (Hoyng et al, 1976). The concept of an elementary flare burst was introduced to account for this cut-off (de Jager and de Jonge, 1978). However, a study by the Hard X-ray Burst Spectrometer (HXRBS) at time resolutions down to 10 ms has revealed significant structure at this level (Kiplinger et al, 1982). Fig.2 shows 22 s of data from a short, intense event on March 22, 1981; the points in Fig.2a are at 128 ms resolution and features are expanded in Fig.2b,c at 30 ms resolution. Spike 1 has a FWHM of 45 ms while spike 4 shows an abrupt (4σ) fall in 20 ms. These X-ray variations are the fastest yet seen from the Sun, although ms fluctuations have been reported at microwave frequencies (Slottje, 1978). Kiplinger et al (1982) note that fast events are rare, with only $\approx 10\%$ of suitable events examined showing fast spikes with durations <1 s. There is lack of such spikes in major events, although this could be a masking effect caused by lack of spatial resolution or an intense, more gradual component. The more intense fast spikes are seen in the presence of a dominating slowly varying component.

One of the most controversial issues regarding the impulsive phase is the thermal/non thermal origin for the hard X-ray bursts. Short decay times place severe constraints on a thermal model; (2.1) and (2.2) show that fast decays are achieved best if either we have a small dimension L in a conduction dominated plasma or a high density in a radiation dominated plasma. In a non-thermal model fast fluctuations are interpreted as bremsstrahlung from electron beams of short duration, conceptually easy to achieve; however the energy conversion efficiency is so small that large numbers of electrons are needed. Nevertheless, SMM results are supporting the non-thermal hypothesis more than the thermal.

Fig.3 displays the intensity-time history of a fast spike event on May 7¹, imaged by HXIS in the 16-30 keV band with 1.5 s resolution. There are two broad peaks, each with significant fine structure at the 1.5 s level; this event also exhibited 60 ms time structure above 29 keV (Kiplinger et al, 1982). Spatial intensity contours are shown at various times within the bursts. The first bursts in the first peak originate in

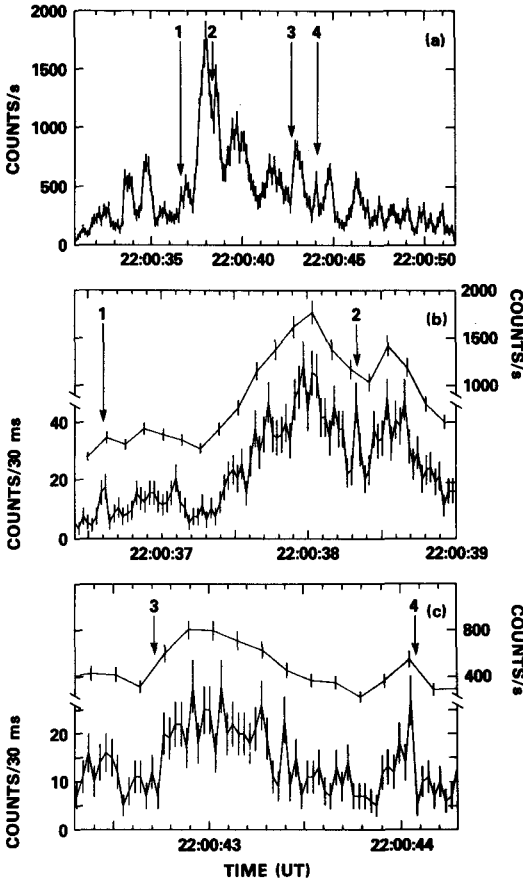


Figure 2. Fast hard X-ray time variations on March 22, 1981. (Kiplinger et al, 1982)

a compact, $<6''$ FWHM, source, which is co-located with the southern-most of two bright H_{α} kernels visible just before the flare. The picture from 14.56.06-14.56.14 covering the last part of the first peak shows an additional component to the north. These two bright points are interpreted as footpoints of a magnetic loop. The small bursts between the two main peaks are from the south footpoint. From 14.56.34-14.56.49, covering the second peak, the emission is diffuse. The halo around the centroid could be Compton backscattering off the photosphere from a hard X-ray source rising in altitude within the loop. During the decay the centroid shifts to midway between the footpoints, consistent with the looptop. Data from the X-ray Polychromator (XRP) (Acton et al, 1982) is interpreted as chromospheric evaporation from the south footpoint, driven by the impact of non-thermal electrons rather than a thermal conduction front.

One of the principal arguments advanced by proponents of thermal models for hard X-ray bursts is that for many flare situations, emission from a thermal plasma is more efficient than bremsstrahlung for a non-

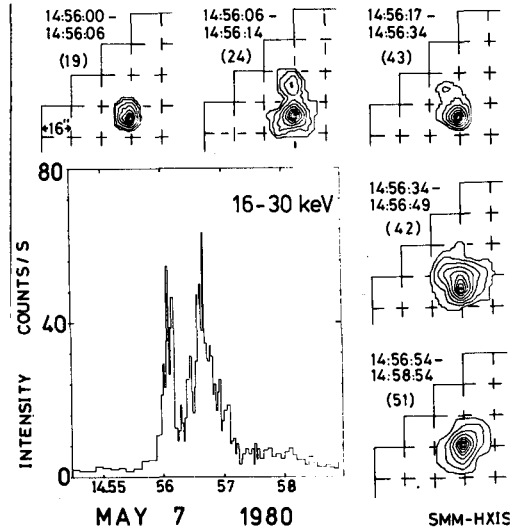


Figure 3. The fast hard X-ray burst on May 7. Contour maps of the flare are given at different times during the bursts. Numbers in parentheses are the maximum intensity (counts) at the peak contour over the accumulation time given.

thermal beam. However, Kiplinger et al (1982) have made a detailed analysis of the May 7 event and have shown there to be no thermal advantage, and have ascribed a non-thermal origin to the fast spikes.

The Gamma Ray Spectrometer (GRS) has observed over 100 flares with emission above its 0.3 MeV threshold with some 30 or so showing evidence for unresolved prompt nuclear de-excitation lines from ^{16}O and ^{12}C at 6.13 and 4.44 MeV respectively (E.Rieger, 1982, private communication). A subset of the latter also show the 2.223 MeV neutron capture line $^1\text{H}(n,\gamma)^2\text{H}$. This is a delayed line for which the neutrons must first slow down and then be captured by ambient protons. Both processes are density dependent, with the capture time dominant. The delay of the 2.223 MeV line from the prompt de-excitation lines is typically ≈ 100 s, which implies (Wang and Ramaty, 1974) that the mean density at which the neutrons are captured is 10^{17} H cm $^{-3}$, or just within the photosphere. Neutrons are produced in the first instance from break-up of the ^4He by protons ≈ 25 MeV, with contributions from spallation of heavier nuclei.

Events such as May 7 show that electron acceleration up to sub-relativistic energies is impulsive. It transpires from other events that this also applies up to at least a few MeV for electrons and many times this energy for ions. In the June 7 event the time history of the gamma ray intensity at the energies of the prompt de-excitation lines discussed above was equally impulsive as, and in phase with, the hard X-ray intensity (Chupp et al, 1981). Detailed analysis, taking into account the time history of the 2.223 MeV line also, showed that energetic protons (≈ 50 MeV) and relativistic electrons (1 MeV) were accelerated in a similar time scale, quite contrary to earlier beliefs.

There have been further developments following a limb flare on June 21, 01.19 UT, when neutrons up to 600 MeV were detected by GRS (Chupp et al, 1982). The timing of the neutrons at 1 A.U. showed that protons up to 1 GeV must have been accelerated coincident with, or within a few seconds of, the impulsive phase. Ion acceleration in this flare must have been efficient, for the 511 keV positron annihilation line was seen. This results from nuclear interactions which produce radio-isotopes such as ^{11}C , ^{13}N , ^{15}O , ^{19}Ne , etc. The positron line has been observed in very few events. High energy neutrons have recently been detected from the June 3, 1982, X8 flare (Forrest, D.J., private communication) showing that the June 7 event was not unique in this solar cycle.

From an overview of the gamma ray events two things emerge: 1) many events are sub-flares when seen in H_α ; 2) de-excitation lines are seen more often than the 2.223 MeV neutron capture line, which itself is more common than the 511 keV line. Thus acceleration of electrons up to 0.5 MeV and protons to a few MeV is both common and part of the impulsive phase. The difference between small gamma ray flares and major H_α flares is that in the latter particle acceleration in the impulsive phase is more efficient and may extend to higher energies. The concept of a two stage acceleration process no longer seems necessary to explain the highest particle energies reached in flares.

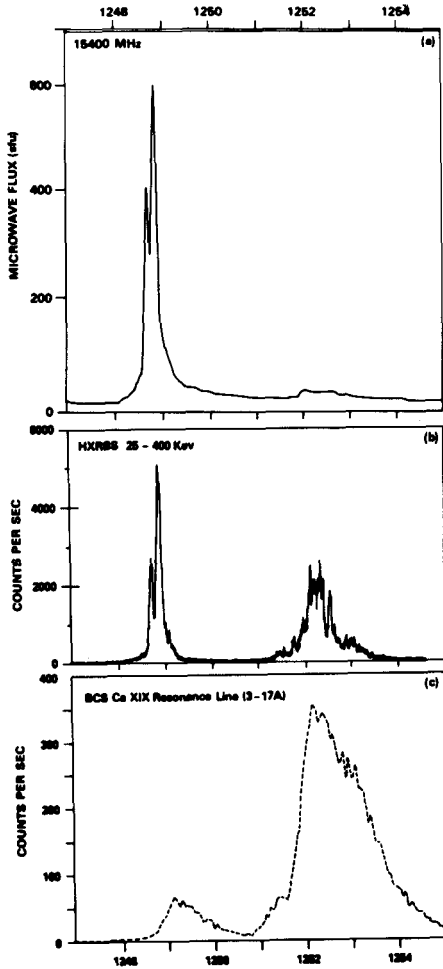


Figure 4. The double flare at 12:48 August 31 (Strong et al, 1982)

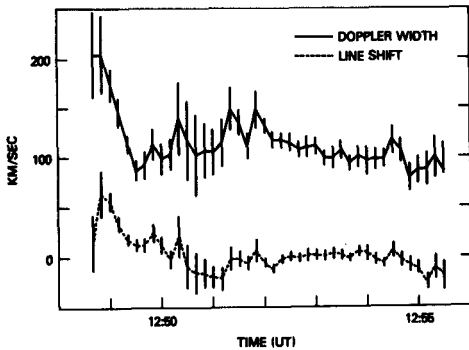


Figure 6. Doppler broadening and blue shift during the double flare on August 31 (Strong et al, 1982)

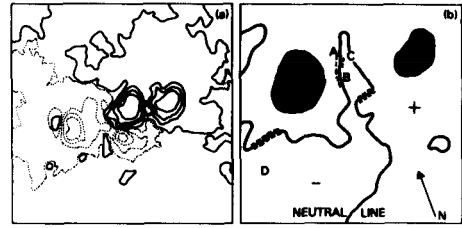


Figure 5 a) the transverse magnetogram on August 31; b) the position of the initial flare brightenings A,B,C. (Strong et al, 1982)

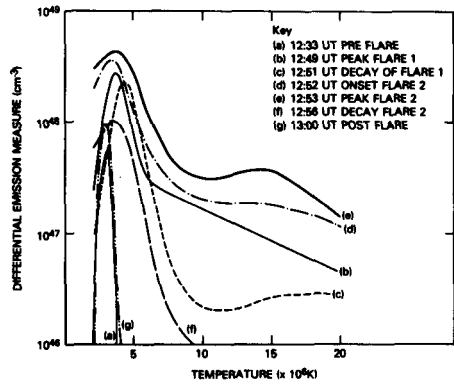


Figure 7. Differential emission measure analysis ($\text{cm}^{-3}/10^6 \text{ K}$) for the double flare on August 31. (Strong et al, 1982)

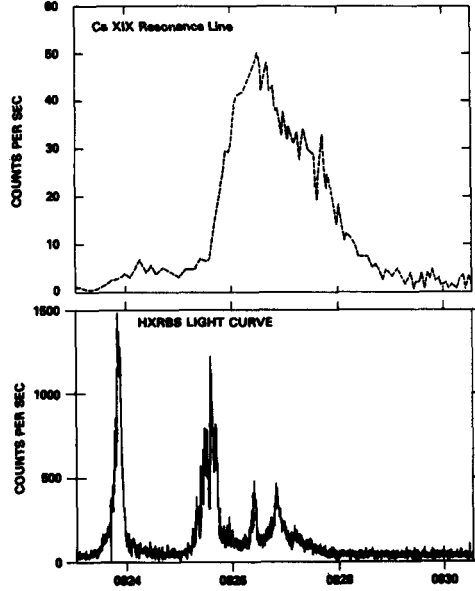


Figure 8. The double flare at 9:24 August 31. (Strong et al, 1982)

We turn now to a compact event, consisting of two closely separated flares, which is illustrative of the co-ordinated analysis possible from SMM and ground based observations. Fig.4 shows the intensity at 15.4 GHz, 25-400 keV and the Ca XIX resonance line from 12.47-12.55 on Aug 31 (Strong et al, 1982). The Ca XIX line is monitored by the Bent Crystal Spectrometer (BCS) of the XRP. The doubly impulsive first flare is very hard with a photon number spectrum obeying $dJ/dE \propto E^{-3}$ up to 150 keV. The microwave profile mirrors that of the hard X-rays (a typical feature) indicating that electrons had access to a region from which microwave radiation was (a) produced and (b) escaped. The soft X-rays (Fig.4c) reached maximum 20-30 s after the hard X-ray peak and exhibited a rapid decay (e-folding time 35 s). Fig.5a shows the longitudinal magnetogram of the flare region where a -ve inclusion is evident between two major +ve sunspots. Fig.5b sketches the region between the +ve spots, showing the locus of the magnetic neutral line; the Ultraviolet Spectrometer and Polarimeter (UVSP) identified the Fe XXI emission at 1354Å at points A, B and C during flare onset. In the impulsive phase of the first event HXIS imaged the 16-30 keV X-rays at two opposite sides of the core of the soft X-ray emission. This is consistent with a flare contained in a magnetic arch, with soft X-ray emitting plasma at the top and hard X-rays produced by electron beams at the footpoints. This model is supported by observations of metric frequency U-bursts.

In the second event a few minutes later the hard X-ray burst is made up of many fast spikes; also the peak in the soft X-ray intensity is co-located with the hard X-ray peak at a point displaced 5" NE of B. The X-ray spectrum from the whole flare has the same slope as for the first flare, but now there is a substantial low energy, thermal component.

The BCS can determine the turbulent velocity of the plasma from the Doppler broadening of the Ca XIX line, and also the bulk motion from the shift in line centre. These parameters are shown in Fig.6. Turbulent velocities reach 200 km/s during the first flare but do not change during the second. The line is quite strongly blue shifted during the first flare but not during the second. Strong et al (1982) concluded that in the second flare, because of the increased density from the earlier event, the non-thermal electrons lose the majority of their energy within the loop, rather than at the footpoints. The density is probably non-uniform throughout the loop so the bulk of the energy dissipation may appear close to a footpoint, from which the plasma will expand to fill the whole loop. If the loop is unresolved, this will manifest itself by a shift in the centroid of the emission, which is in fact seen. It is difficult to distinguish between lateral and vertical motion as the flare was at N12 E31 and the apparent motion is \approx NE.

The Flat Crystal Spectrometer (FCS) of the XRP investigated the multithermal nature of the coronal plasma throughout the flares (Strong et al, 1982). A differential emission measure analysis is shown in Fig.7 for seven times during the flares. The plasma state both pre-flare and post-flare appears isothermal while during the flares there is an enhanced high temperature component which has a significantly higher emission measure for the second flare than for the first.

A few hours before the Aug 31 event a weaker but similar pair of compact flares had occurred in the same region. The hard and soft X-ray time histories are shown for comparison in Fig.8. The common features are the first fast impulsive event, with low soft X-ray emission and a second multiple spike hard X-ray burst associated with a more dominant soft X-ray peak. The decay times are similarly fast. The main difference is that the soft X-rays peak significantly after the hard X-ray burst; this is interpreted as a lack of significant expansion of material into the loop following the first event, thus depriving the loop of sufficient stopping power for the second hard X-ray burst.

Events following this pattern may be very common, as may be seen from Fig.9, which shows HXIS data from a flare on October. 20. The initial impulsive hard X-ray peak is followed 1 m later by a longer, weaker peak. At 3.5-5.5 keV the slowly rising weak first event merges with the more intense second event, which like Aug 31 peaks approximately simultaneously with the hard X-rays. The soft X-rays have a fast, 30 s e-folding decay. Inset in Fig.9 is the hard X-ray contour map at the time of the first peak. The two clearly resolved features separated by $\sim 20''$ are suggestive of magnetic loop footpoints. During the second peak only the easterly point is bright, both at 3.5-5.5 keV and 16-30 keV. This event is similar to that on May 7 (Fig.3) with visible footpoints during the first burst and emission from one point during the second burst. Projection effects due to the easterly location of the October 20 flare mean the coincidence of the second burst with the easterly footpoint could also arise if the emission was from the looptop.

To summarise, there is a class of flare with two major energy releases in a region containing a compact magnetic loop; the hard X-ray data show considerable structure within each energy release, the first of which often causes chromospheric evaporation. The subsequent evolution depends on how the effects of the first release change the plasma state within the loop. The second release always appears dominant at soft X-ray wavelengths and rarely is resolved as a second footpoint.

Until SMM the existence of electron beams at the onset had not been proved. One of the first major results (Hoyng et al,1981) identified the points of impact of such beams on the chromosphere from a large 2-ribbon flare on May 21. UVSP observed the flare in the Mg II line at 2795\AA , and demonstrated coincidence in space and time between the hard X-ray and UV bright points and H_{α} kernels. After the impulsive phase the centroid of the X-ray emission at both hard and soft wavelengths was at the looptop between the footpoints. Duijveman et al (1982) have analysed this and two other large events for which footpoint emission was seen in the impulsive phase. They show that the near simultaneous brightenings cannot be accounted for by an MHD disturbance triggering one source from the other for any reasonable values for magnetic field and plasma density. The number of electrons in each beam >16 keV in these large flares is in the region $10-30 \times 10^{36}$, and the energy in each beam is $2-9 \times 10^{29}$ erg. This is small compared with the total flare energy estimated at the peak of the thermal phase. Some large flares also show the double structure summarized above for the small compact flares.

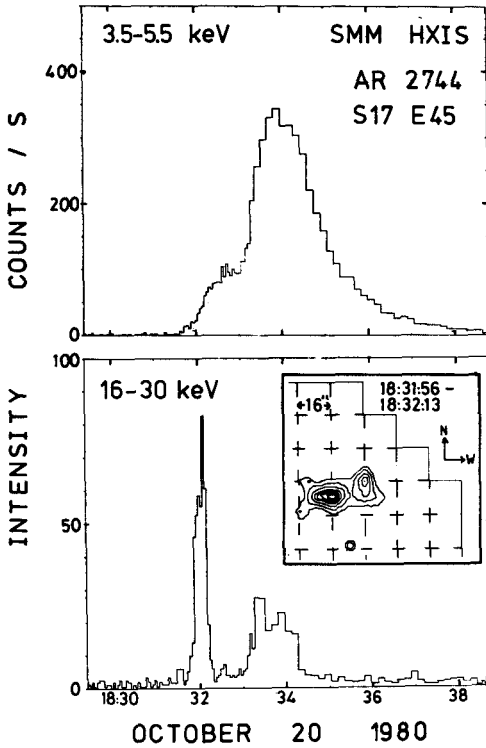


Figure 9. The double flare at 18:32 October 20. Inset is the hard X-ray contour map during the first spike.

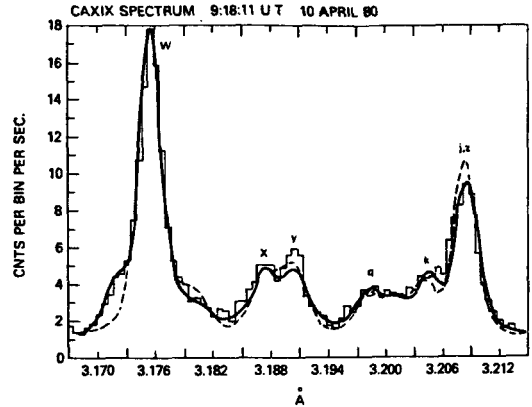


Figure 10. The Ca XIX spectrum at the hard X-ray maximum of the April 10 flare. (Antonucci et al, 1982)

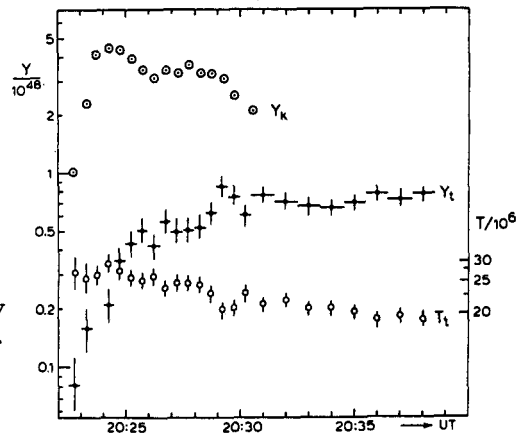


Figure 11. The emission measure of the kernel, Y_k and the tongue, Y_t of the limb flare at 20:25 April 30. Also shown is the electron temperature T_t of the tongue (de Jager et al, 1982)

SMM has studied the dynamics of the flare plasma in unprecedented detail. During the impulsive phase of large flares, the plasma exhibits characteristic turbulence and upward motion, the latter frequently reaching $300\text{--}400 \text{ km s}^{-1}$ (Antonucci et al, 1982). Fig. 10 shows the Ca XIX spectrum during the impulsive phase of the April 10 flare. The spectrum shows not only a non-thermal broadening, best seen in the resonance line w but also a well defined blue wing. The theoretical stationary spectrum is shown dotted, and the solid line is obtained by adding a blue shifted component to it. Antonucci et al have computed the heat content and kinetic energy of the upward moving chromospheric plasma and have shown this to be sufficient to account for the energy contained in the flare loop during the main phase. It is well in excess of the energy in the electron beam deduced from an analysis of the hard X-ray burst using a thick target hypothesis (Duijveman et al, 1982). The additional energy is probably supplied by ions accelerated with the electrons. The ions are invisible

until they reach energies of several MeV/nucleon, when they start exciting nuclei, with resultant gamma ray emission; yet the spectrum below this threshold can easily contain the bulk of the flare energy.

Poland et al (1982) and Woodgate et al (1982) have reported coincidence between the impulsive hard X-rays and brightening in the OV line (1371Å) formed primarily in the transition zone at 2.5×10^5 K. This is seen for both limb and disc flares, and leaves little doubt that the emissions come from loop footpoints. The good spatial resolution of UVSP allowed impulsive excitation from the limb event at 18:23 on June 29 to be tracked up to 30,000 km into the corona, indicating that rapid evaporation follows the impulsive phase (Poland et al, 1982). They saw material ejected into the flare loop and a more open coronal structure. The X-ray bursts with the hardest spectra appeared in coincidence with features within the closed loop, where the density is relatively high.

Unlike disc flares, the morphology of limb flares can be examined unambiguously by the imaging instruments. De Jager et al (1982) have shown in the thermal phase of the April 30 flare that while the majority of the X-ray and UV emission was confined to a relatively compact low lying loop, electrons escaped from this loop to populate a much larger structure extending to at least 80000 km into the corona. Fig.11 shows the time history of the emission measure from the main flare and the coronal "tongue", and the electron temperature of the tongue, which initially is higher than the flare kernel. This indicates that only the higher energy electrons escape from the main loop.

Limb flares regularly show large coronal structures which provide a link between widely separated active regions. As the density decreases such structures tend to become invisible, so the observations only give a lower limit to their true altitude. Following the Nov 6 east limb flare (Svestka et al, 1982a) an arch was visible to $\approx 1.5 \times 10^5$ km; a similar large arch was also imaged in soft X-rays after the May 21 flare (Svestka et al, 1982b) and the June 29 flare. In June the link between the active regions, 2522 and 2530 ($\approx 1.5 \times 10^5$ km apart) was established while they were still well on the disc. Some flares from these regions produced time coincident (within ≈ 1 m) sympathetic events in the other region, regardless as to which region flared first. At quiet times there was frequent evidence for a soft X-ray bridge between the two regions. Other regions, such as 2370 and 2372 in April were similarly connected, so this must be regarded as a normal state on the Sun.

Flares which occur within such a connection are likely to populate the high arch with trapped particles. Such events are therefore invariably associated with metric radio noise storms from the trapped electrons. One of the most interesting features on Nov 6 was a quasi-periodic variation (≈ 20 m) in soft X-rays with no response in the chromosphere ($H\alpha$) and little in the OV transition region line (Svestka et al, 1982a). Thus the energy source was not from fresh small flares; it was presumably from dumping of trapped particles from the corona to a denser part of the atmosphere, similar to a terrestrial aurora. In the solar case the ions

are the more likely species to cause the X-ray emission via local heating at the top of the chromosphere.

The corona is playing an ever important role in flare studies. During the early stages of some flares, Benz et al (1983) found that decimetric and soft X-ray emission was observed prior to both the impulsive flash phase and the gradual pre-flash phase as seen in X-rays >26 keV. Significantly, the locations of the Type III bursts in these events are not all the same, indicating that energetic electrons are present prior to the main flare. In some events there is evidence for a reverse drift metric burst prior to the flare, indicating that some electrons are moving downwards. Benz et al conclude that in such events energy carried by the downward moving particles may provide the flare trigger.

There are other interesting aspects to the SMM data. One feature of many active regions, such as AR 2372 in April, is the production of homologous flares, indicating a certain stability in the dominant magnetic structure, despite the instabilities inherent in the flare process. In fact, even flares from different regions may have many similarities as we have seen. The general magnetic field topology may be identical for all these flares and differences between flares may represent trivial variations in dimension and field magnitude that alter the final appearance of the flare out of all proportion.

In sunspot studies Gurman et al (1982) have reported transition region oscillations in the umbra with typical periods in the 2-3m region. Peak intensity is in phase with the maximum blue shift and they interpret the oscillations as upward propagating acoustic waves. The energy flux, however, at $\leq 2 \times 10^3$ erg cm⁻²s⁻¹ is 10^7 too small to account for the missing sunspot radiative flux. The global effect of the latter has been demonstrated by the Active Cavity Radiometer (Willson et al, 1981). They showed the Solar Constant to have variations as high as -0.2%, due apparently to the presence of large sunspot groups. This energy must ultimately be released, probably in white light faculae; however, lack of significant high frequency fluctuations, <7 days, suggests that the missing energy must be stored in the convection zone for ≥ 7 days.

The remaining instrument on SMM was the Coronagraph/Polarimeter, which did not observe the Sun directly. However, in terms of energy release in flares, it is evident that the corona plays a major role. Detailed analysis by Wagner et al (1981) concluded that the mechanical energy in a coronal transient may exceed the total radiated flare energy by over an order of magnitude. Thus the least visible of solar events turns out to be the most energetic! If this is true in flare stars, then individual events release a prodigious amount of energy. As the transient moves outwards it becomes supersonic, generating an interplanetary shock, and indeed it has been shown that most, if not all, of such shocks are initiated by a coronal transient.

4. SUMMARY

The advances made in the study of solar flares could help us to a better understanding of red dwarf flare stars. Before drawing too many parallels,

however, we must remember that differential solar rotation and the dynamics of the convection zone are intimately related to sunspot and flare activity; flares are almost perfectly correlated with sunspots and there have been times in history when sunspots disappeared for long periods. Very little is known about the corresponding phenomena on flare stars, so the flare mechanism might be quite different. Scaling from solar flares to red dwarf flares may be inappropriate at worst, difficult at best. A decisive datum would be the observation of the separate impulsive phase in a stellar flare, but for this we must await more sensitive hard X-ray instrumentation.

ACKNOWLEDGEMENT

The author expresses his deepest thanks to members of the SMM experiment teams for supplying material used in this review.

NOTE¹ Unless otherwise stated all flares are 1980

REFERENCES

- Acton, L.W. et al, 1982: Ap.J. (to be published)
 Antonucci, E. et al, 1982: Solar Phys. 78, 107
 Benz, A.O. et al, 1983, Solar Phys. 83, 267.
 Chupp, E.L. et al, 1981: Ap.J.Lett, 244, L171
 Chupp, E.L. et al, 1982: Submitted to Ap.J.Lett.
 Crannell, C.J. et al, 1978: Ap.J. 223, 620
 de Jager, C and de Jonge, 1978: Solar Phys. 58, 127
 de Jager, C. et al, 1982: Submitted to Solar Phys.
 Duijveman, A. et al, 1982: Solar Phys. 81, 137.
 Gurman, J.B. et al, 1982: Ap.J. 253, 939
 Haisch, B.M. et al, 1980: Ap.J.Lett. 242, L99
 Hoyng, P. et al, 1976: Solar Phys. 48, 197
 Hoyng, P. et al, 1981: Ap.J.Lett. 246, L155
 Jarrett, A.H. and Gibson, J.B. 1975: IBVS, No.979
 Kahler, S. and Shulman, S. 1972: Nature Phys. Sc. 237,101
 Kahn, S.M. et al, 1979: Ap.J.Lett, 234, L107
 Kiplinger, A.L. et al, 1982: Submitted to Solar Phys.
 Kunkel, W.E., 1969: Nature, 222, 1129
 Kunkel, W.E. 1975: I.A.U. Symposium No.67, 15
 Lin, R.P. and Hudson, H.S. 1976: Solar Phys. 50,153
 Moore, R.L. et al, 1980: In "Solar Flares", Colorado Ass.Univ.Press
 Mullan, D.J. 1976: Ap.J. 207, 289 (Ed.P.Sturrock)
 Mullan, D.J. 1976: Ap.J. 207, 289
 Poland, A.I. et al: 1982: Solar Phys. 78, 201
 Simnett, G.M. 1981: Proc. 17 Int.Conf.on Cosmic Rays, Paris, Vol.12,205
 Slottje, C. 1978: Nature Phys. Sc. 275, 520
 Strong, K.T. et al, 1982: Submitted to Solar Phys.
 Svestka, Z. et al, 1982a: Solar Phys. 75, 305
 Svestka, Z. et al, 1982b: Solar Phys. 78, 271.
 Wagner, W.J. et al, 1981: Ap.J.Lett. 244, L123
 Wang, H.T. and Ramaty, R, 1974: Solar Phys. 36, 129
 Willson, R.C. et al, 1981: Science, 211, 700
 Woodgate, B.E. et al, 1982: Submitted to Ap.J.

DISCUSSION

Stencel: I would like to ask about the flare events. In the second peak always the brightest and if so could this be a reflection with argumentation? Secondly, does the 30 msec timescale reflect something fundamental about spatial structure?

Simnett: The relative brightness of the peaks in double flare events is a function of wavelength. At microwave frequencies and in hard X-rays the first peak is almost always the biggest (Figure 9). Indeed there are some flares where the first peak is only seen in hard X-rays. Vice versa is true for soft X-rays. The model I outlined agrees quite well with this. The energy release from the first flare goes into particles which then gradually heat the medium, evaporate material which they continue to heat. This heated material then expands producing the soft X-rays. Whether the 30 msec interval is fundamental or not is not clear at this stage. You may recall the results of de Jager, de Jong and the Utrecht group based on the TD-1 data which concluded that there was no significant variation on timescales shorter than 1 second. This was due to their poorer time resolution. This result now revises this conclusion. But I should warn that the time resolution here is only 10 msec and variations are seen down to this timescale. So it is not clear whether the 30 msec timescale is fundamental or not. I should add to that the microwave people see variations at the msec level and so I would suspect that, when X-ray time resolution gets down to that, they may see the same thing.

Hartmann: When you say that solar flares are longer in duration than stellar flares, are you comparing events of comparable energy?

Simnett: No. Of course I cannot compare events of comparable energy because most of the stellar flares for which I have data are considerably in excess of a few time 10^{32} ergs which is the energy of the largest solar flares. The largest flares tend to go for an hour or so and I believe that this is a fairly general rule.

Venugopal: Are you sure about the reduction of the solar constant during a large spot? Is there a quantitative relationship between the two effects?

Simnett: No, there does not appear to be a quantitative relationship between the two. I say this because there were times when there were large spots on the Sun and the reduction in intensity was not very significant. What I am saying is that the two biggest dips in overall solar intensity were coincident with the passage of large spots. I leave you to interpret that how you will.

Venugopal: Can you elucidate the response characteristics of active (word lost) radiometer?

Simnett: Let me discuss this with you later. It is a bit detailed for now.

Linsky: One thing which is very hard to measure in stellar flares is velocity fields or the kinetic energy of gas motions. Could you tell us what SMM tells us about velocities of expansion and the fraction of the total energy going into kinetic motion of gas in the case of solar flares? Do you know what the kinetic energy is and can you compare it with kT ?

Simnett: Let me answer that in a slightly different way. One of the instruments from which I did not show any data is the coronagraph which has seen frequent coronal transients. Calculations of the energy in these measured at a couple of solar radii is typically a factor of 10 greater than the total radiated energy of the corresponding flare. So to answer your question, the dominant energy transfer would appear to be in the mass motion associated with the coronal transients.

Vaiana: I think it is also important to know what fraction of the flares seen by SMM have coronal transients associated with them. Skylab results suggested that there were in fact two types of solar flares. In one type there was no need to invoke mass motions except in the filling of a loop.

Simnett: Perhaps I can answer this in a qualitative way since a great deal of analysis still remains to be done. It looks as though the compact flares, which are intimately related to large scale magnetic structures linking the flaring region to another separate region, are not associated with coronal transients. On the other hand, the flares, even relatively minor ones, which are associated with much bigger structures often seen linking several active regions, were seen by the coronagraph polarimeter to frequently give rise to coronal transients. So you are correct. To say there are two types of flare only may be over-simplifying the matter but it is certainly true that there are at least two types of flare. In one type coronal transients are generated, and these are very common, while the other type are the compact flares.

Vaiana: (Part of question lost). I do not remember the exact statistics but I thought that from Skylab data mass-loss events were relatively rare although they were very significant in terms of total energy.

Simnett: Well, all of the SMM data has not been processed yet so I think we must wait perhaps another year before we can discuss the statistics with confidence. It is actually quite difficult for the coronagraph to observe transients from flares which are well into the disk.

Gibson: I have two questions. Were there any radio observations simultaneous with the pulsational gamma-rays?

Simnett: Yes.

Gibson: Did they show pulsations also?

Simnett: They did yes.

Gibson: This causes me at least to rethink the possibility that in stars the pulsations might be due to the particle distribution rather than some narrow-band phenomenon. I believe it is important that we begin to look at ways of generating particles in pulses rather than some peculiar arrangement of the fields such that a narrow beam passes through the line of sight.